PAIN® 154 (2013) 110–118

www.elsevier.com/locate/pain

Quantitative cerebral blood flow mapping and functional connectivity of postherpetic neuralgia pain: A perfusion fMRI study

Jing Liu [a,1], Ying Hao [b,1], Minyi Du [c], Xiaoying Wang [a,b,*], Jue Zhang [b,d,*], Brad Manor [b,e], Xuexiang Jiang [a], Wenxue Fang [c], Dongxin Wang [c]

[a] Department of Radiology, Peking University First Hospital, Beijing, China
[b] Academy for Advanced Interdisciplinary Studies, Peking University, Beijing, China
[c] Department of Anesthesiology, Peking University First Hospital, Beijing, China
[d] College of Engineering, Peking University, Beijing, China
[e] Division of Gerontology, Beth Israel Deaconess Medical Center, Harvard Medical School, Boston, MA, USA

Sponsorships or competing interests that may be relevant to content are disclosed at the end of this article.

ARTICLE INFO

Article history:
Received 30 April 2011
Received in revised form 12 August 2012
Accepted 29 September 2012

Keywords:
Arterial spin label
Cerebral blood flow
Postherpetic neuralgia
Regional CBF
Seed-based correlation analysis
Striatum

ABSTRACT

This article investigates the effects of postherpetic neuralgia (PHN) on resting-state brain activity utilizing arterial spin labeling (ASL) techniques. Features of static and dynamic cerebral blood flow (CBF) were analyzed to reflect the specific brain response to PHN pain. Eleven consecutive patients suffering from PHN and 11 age- and gender-matched control subjects underwent perfusion functional magnetic resonance imaging brain scanning during the resting state. Group comparison was conducted to detect the regions with significant changes of CBF in PHN patients. Then we chose those regions that were highly correlated with the self-reported pain intensity as "seeds" to calculate the functional connectivity of both groups. Absolute CBF values of these regions were also compared across PHN patients and control subjects. Significant increases in CBF of the patient group were observed in left striatum, right thalamus, left primary somatosensory cortex (S1), left insula, left amygdala, left primary somatomotor cortex, and left inferior parietal lobule. Significant decreases in CBF were mainly located in the frontal cortex. Regional CBF in the left caudate, left insula, left S1, and right thalamus was highly correlated with the pain intensity, and further comparison showed that the regional CBF in these regions is significantly higher in PHN groups. Functional connectivity results demonstrated that the reward circuitry involved in striatum, prefrontal cortex, amygdala, and parahippocampal gyrus and the circuitry among striatum, thalamus, and insula were highly correlated with each element in PHN patients. In addition, noninvasive brain perfusion imaging at rest may provide novel insights into the central mechanisms underlying PHN pain.

1. Introduction

Living with chronic pain negatively impacts one's quality of life [1,4]. Peripheral neuropathic pain most frequently originates from injury or dysfunction of peripheral nerves. Recently, it has also been linked to changes in the connections among central neurons [6,41]. Postherpetic neuralgia (PHN) is a common type of neuropathic pain caused by reactivation of the varicella zoster virus. Similar to other chronic neuropathic conditions, patients with PHN show multiple signs of both peripheral and central neuropathy [28]. Yet, because few studies have explored the effects of PHN pain on brain activity [14,19], the effects of PHN pain on brain network arrangement and function are poorly understood.

Cerebral blood flow (CBF) is believed to be strongly associated with cerebral metabolism. Thus, examining changes in regional CBF (rCBF) over time has been used extensively in pain studies to map neural pathways [3,31,32]. rCBF can be quantified directly using arterial spin labeling (ASL) magnetic resonance imaging (MRI) [47,48]. Recent advances in MRI technology, including greater magnetic field strengths and improved phased array receiver coils [40,43], have increased the sensitivity of ASL, making it a realistic option for functional studies of pain [30,31].

ASL MRI can be applied to investigate both static and dynamic CBF characteristics in a single session within the same subject [48]. Static CBF is quantified by voxel-wise averaging of CBF values over the time domain and can be used to examine rCBF changes.

* Corresponding authors. Addresses: Department of Radiology, Peking University First Hospital, No. 8, Xishiku Street, Xicheng District, Beijing 100034, China. Tel.: +86 10 83572097; fax: +86 10 66551108 (X. Wang), Academy for Advanced Interdisciplinary Studies, Peking University, Beijing 100871, China. Tel.: +86 10 62755036 (J. Zhang).

E-mail addresses: cjr.wangxiaoying@vip.163.com (X. Wang), zhangjue@pku.edu.cn (J. Zhang).

[1] These authors contributed equally to this paper.

0304-3959/$36.00
http://dx.doi.org/10.1016/j.pain.2012.09.016

Dynamic CBF analysis uses the cross-correlation between regions—in this case, the regions involved in pain—to examine the brain circuitry for processing specific pain information.

Several studies [3,29] have indicated that pain is processed in a distributed cortical network. However, the regions involved may be dependent on the specific type of pain [3,29]. Furthermore, information processing between 2 cortical areas may induce functional connectivity [35], suggesting that the cortical areas involved in the processing of pain may be functionally connected. Thus, we aimed to identify the cortical network involved in the processing of PHN pain, as well as the effects of this chronic neuropathic condition on functional connectivity as measured by resting-state brain activity. We hypothesized that compared with control subjects, PHN patients would demonstrate a unique pattern of rCBF that was highly correlated with self-reported pain intensity and internally connected by a single functional network.

2. Materials and methods

2.1. Ethics statement

This study was approved by the local ethics committee, and all subjects provided informed written consent, in line with the Declaration of Helsinki.

2.2. Subjects

Seventeen right-handed PHN patients admitted to the Peking University First Hospital Pain Clinic were recruited, of which 11 were eligible: all male patients age 59 to 73 years (mean 66 years). All participants reported a history of shingles, associated severe pain, and varicella zoster virus infection. PHN pain was localized in the left side of the body in 9 cases and the right side for 2 cases. All participants reported a history of persistent pain for at least 2 months after resolution of the acute shingles episode, with a pain intensity of at least 7 of 10 on a mechanical visual analog scale (VAS) (a measurement of pain intensity ranging from 0 to 10, with 0 meaning no pain and 10 meaning highest tolerable pain) [20]. Pain level was also assessed immediately before the functional MRI (fMRI) to ensure that participants were experiencing moderate to severe pain (ie, VAS $\geqslant 6$) during the experiment. Participants also completed standard neurological and psychological examinations, as well as standard anatomical brain MRI. Neurological examination consisted of assessments for consciousness, thinking, speaking, cranial nerve function, motor control (ie, muscle strength, muscle tone, and coordination), reflexes (ie, tendon reflex, pathological reflex), and sensation (ie, decrease or absent). The psychological examination consisted of the Mini-Mental State Examination [13].

Seven participants had prescriptions for analgesic medication such as oxycodone and/or propionic acid. Participants suffering from significant psychiatric disorders and/or brain structural abnormalities were excluded in our study. Four participants suffered from slight insomnia, and 3 of these participants were prescribed diazepam. Medications were withheld the day before and on the day of examination.

Eleven age-matched right-handed healthy male subjects were recruited as control subjects (age 56 to 73 years, mean 64 years). None suffered from any type of chronic pain, psychiatric disorders, or brain structural abnormalities, and none were taking medications that may have altered brain activity.

2.3. Data acquisition

During all brain scans, subjects were instructed to stay awake with their eyes closed and minds clear. Maximum care was taken to avoid situations that may trigger abnormal pain. fMRI was performed on a 3T Signa Excite HD scanner (GE Medical Systems, Milwaukee, WI) with an 8-element, receive-only head coil. Subjects laid in a supine position on the scanner table with head immobilized by foam padding. High-resolution anatomical images were first acquired using a 3-dimensional gradient-echo T1-weighted sequence (180 transverse slices, repetition time (TR)/echo time (TE): 25/4 ms; field of view (FOV): 230 mm^2; slice thickness: 2 mm with no gap). Anatomical images were utilized for registration of the functional images, as well as for anatomical atlas transformation.fMRI data were acquired for 8 consecutive minutes using a dual-echo spiral-out pulsed ASL sequence that interleaves pulsed ASL acquisitions with slab-selective and nonselective inversion using PICORE (proximal inversion with a control for off-resonance effects) tagging [44] and QUIPSS II (quantitative imaging of perfusion using a single subtraction). PICORE/QUIPSS II applies saturation pulses to the tagging region to control the time duration of the tagged bolus. QUIPSS II renders the pulsed ASL technique relatively insensitive to transit delays and thus ensures accurate quantification of perfusion [24,45]. The readouts utilized a slice thickness/gap of 8.0/2.0 mm with 2.9×2.9 mm^2 in-plane resolution, using a 230 mm^2 FOV with 64×64 acquisition matrix, a TR of 3000 ms, a TE1 of 3.1 ms, an inversion time (TI) of 1.5 seconds, and a 90° flip angle. After inversion, the time of the saturation pulse was 700 ms, with an 800 ms delay between saturation and excitation. Twelve axial slices were placed to cover the entire cerebrum and most of the cerebellum. The set consisted of 160 functional contiguous axial images.

2.4. Data preprocessing

fMRI preprocessing was performed with Statistical Parametric Mapping software (SPM5, Wellcome Department of Imaging Neuroscience, University College, London, UK) and ASLtbx (http://www.cfn.upenn.edu/~zewang/ASLtbx.php) based on SPM5.

For each subject, data were motion corrected using the realignment function in SPM5. Sinc interpolation of the ASL time course was then used to create time-matched control and label images, followed by subtraction to suppress BOLD contamination [2,25]. Absolute CBF image series were generated based on a single-compartment continuous ASL perfusion model utilizing ASLtbx [42]. Functional images were reoriented with the origin at the anterior commissure before being coregistered with the corresponding anatomical image. This technique facilitates transformation to the Montreal Neurological Institute T1 template and resampling of functional images to isotropic $2 \times 2 \times 2$ mm^3 voxels. Functional data were smoothed using a Gaussian kernel of full-width half-maximum 8 mm. Finally, the functional data were detrended linearly and filtered using a bandpass filter (approximately 0.01 to 0.04 Hz).

2.5. Experimental procedure

The statistical analysis consisted of 2 primary steps. First, we determined the effects of PHN on rCBF. Second, we examined the functional connectivity between pain-related regions, as identified in step 1, to determine their interconnectivity and elucidate the underlying circuitry involved in PHN pain (experiment flowchart in Fig. 1).

2.6. Statistical analysis

The mean CBF images for each subject were averaged using Matlab 7.0. To first prove the feasibility of the ASL technique for quantifying static CBF, we computed CBF in the control group within those anatomical regions of interest (ROIs) (based on the

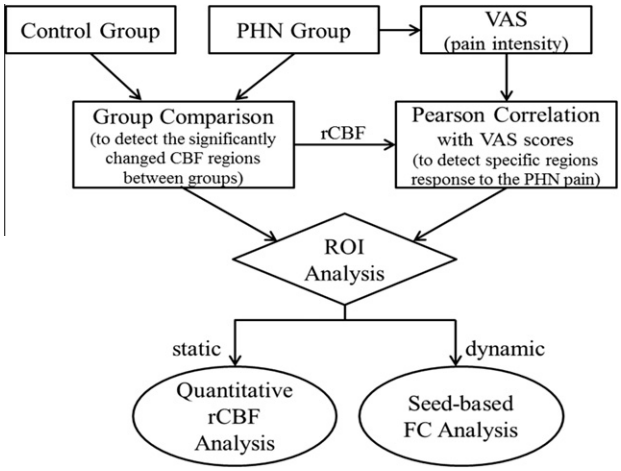

Fig. 1. Flowchart of experiment protocol. PHN = postherpetic neuralgia; VAS = visual analog scale; CBF = cerebral blood flow; rCBF = regional cerebral blood flow; ROI = region of interest; FC = functional connectivity.

Anatomical Automatic Labeling (AAL) template) associated with the default mode network system, including the bilateral posterior cingulated cortex (PCC), precuneus, medial prefrontal cortex (MPFC), parietal lobe, thalamus, and insula/superior temporal gyrus (STG). Each regional value was divided by the subject's global mean CBF to acquire relative rCBF values. Then, a 1-tailed, 1-sample Student *t* test was performed on these relative CBF values against 1 to reveal which brain regions were occupying significantly higher CBF at rest.

Group comparison of the global mean CBF was conducted by a 2-sample *t* test in SPM5. Areas of significant increase or reduction were identified at the cluster level for corrected $P < .05$ (voxel level uncorrected $P < .005$), and a minimum cluster extent size of 10 contiguous voxels was applied.

2.7. Quantitative analysis in global and regional CBF changes

The global mean CBF values for each subject were also calculated for group comparison using a 2-sample *t* test with SPSS 18.0. It has been demonstrated that thalamus, cingulated cortex, insula, primary and secondary somatosensory cortices (S1/S2), and basal ganglia are the common pain-related regions [3,9]. According to the results of group CBF image comparison, pain-associated CBF increases in the patient group were located in the left caudate head, left S1, left insula, and right thalamus. Thus, an ROI analysis was conducted on these regions. The raw CBF values (denoted as absolute CBF) of the regions [37] were calculated for each subject. For each subject, the quantitative CBF values in each ROI were determined by using the SPM Marsbar toolbox.33.

2.8. Correlation analysis between regional CBF values and VAS scores

To determine whether the pain-related regions were correlated with pain intensity, Pearson correlation analyses between regional CBF values and VAS scores were conducted on all of the significant results survived in group CBF comparisons using SPSS 18.0.

2.9. Seed-based correlation analysis (SCA)

Seed-based correlation analysis (SCA) was used to evaluate the dynamic characteristics of CBF and to examine functional brain connectivity in the PHN cohort by group comparison. Brain ROIs were selected according to the results of group ROI analysis. These ROIs were defined in the central coordinates with a 4-mm radius.

After seed selection, mean CBF time courses were calculated. A cross-correlation coefficient map was plotted by correlating the average time course of the seed region with the time course of each voxel in the brain. Six head motion parameters were regressed out. Individual subject-level maps were plotted by converting correlation coefficients to z-scores using Fisher r-to-z transformation. Finally, the results of each group were produced using 1-sample *t* tests to determine whether the z-scores significantly differed from zero. The differences between the 2 groups then were analyzed using a 2-sample *t* test.

Statistical testing in SPM5 was used to identify regions throughout the brain with statistically significant correlation to the seed regions. For the difference between patients and control subjects, cluster level corrected $P < .05$ (voxel level uncorrected $P < .005$) and contiguous voxels >10 were selected. T-score maps were used for intersubject evaluation of CBF results.

3. Results

3.1. Feasibility of quantitative static CBF map

A static CBF map acquired with the pulsed ASL technique in a representative control subject is shown in Fig. 2. Consistent with previous CBF studies [12], in the healthy control, static CBF in the default mode network, including the bilateral PCC/precuneus (relative CBF = 1.432, $P < .001$), MPFC (relative CBF = 1.273, $P < .001$), thalamus (relative CBF = 1.178, $P = .001$), and insula/STG (relative CBF = 1.247, $P < .001$), was greater than the whole brain mean CBF in healthy control subjects.

3.2. The effects of PHN on rCBF

In the patient group, 6 subjects were excluded from the analysis; 1 female subject presented with obsolete parietal lobe infarction and the other 5 (2 female and 3 male subjects) had excessive head motion as defined as more than 2 mm of translation or 2 degrees of rotation in any plane. Clinical characteristics of pain are summarized for the participants in Table 1.

As compared with control subjects, PHN patients demonstrated increased CBF within hedonic regions (ie, the left striatum including the caudate head and lentiform nucleus), sensory regions (ie, the right thalamus and left S1), motor regions (ie, the left primary motor cortex [M1]), and affective regions (ie, the left insula and left amygdala) (details in Table 2 and Fig. 3). CBF was also increased within several subregions of the left inferior parietal lobule (IPL), including the left supramarginal gyrus and left angular gyrus, right fusiform gyrus, bilateral STG, and middle temporal gyri. Conversely, CBF was decreased within the bilateral frontal cortices and the right IPL (ie, the right supramarginal gyrus and right angular gyrus) in PHN patients as compared with control subjects (details in Table 3 and Fig. 3).

3.3. Relationships between rCBF and self-reported pain

Of those regions in which static CBF was altered in PHN patients as compared with control subjects (Table 2), CBF within only 4 regions correlated with VAS pain scores. It was revealed that absolute CBF values of the 4 regions including left S1 (−34, −24, 40) ($r = 0.794$; $P = .004$), left insula (−36, 4, 8) ($r = 0.837$; $P = .001$), right thalamus (18, −6, 12) ($r = 0.799$; $P = .003$), and left caudate head (−14, 24, 2) ($r = 0.725$; $P = .012$) were all correlated with VAS scores with statistical significance ($P < .05$) (Fig. 4A–D).

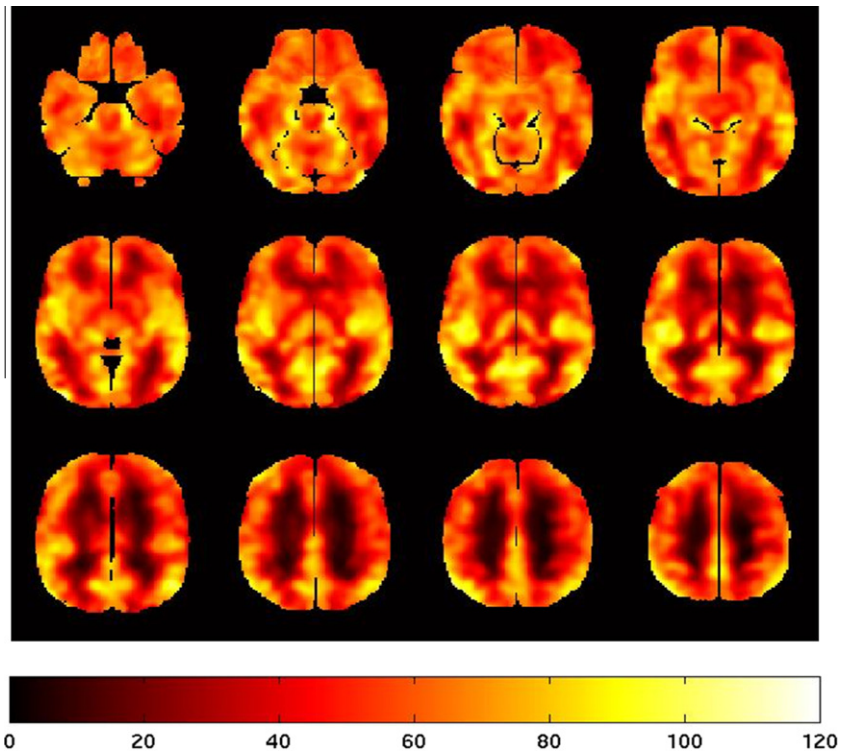

Fig. 2. Mean resting state cerebral blood flow images from a representative control subject. Images were averaged across all cerebral blood flow images acquired during resting state from a healthy male. Twelve axial slices were collected. The scale is given in units of mL(blood)/100 g(tissue)/min.

Table 1
Clinical characteristics of patients with postherpetic neuralgia.

Patients	Age (y)/ gender	Location of lesion	Pain duration	Visual analog scale
1	70/M	Left T3-T5	6 mos	9
2	71/M	Left T6-T10	3 mos	7
3	71/M	Left L2-L3	8 mos	9
4	59/M	Left T2-T5	2 mos	7
5	73/M	Left T3-T5	2 y	8
6	73/M	Left T7-T11	11 mos	7
7	62/M	Left T6-T8	6 mos	8
8	66/M	Left T2-T9	1.2 y	8
9	59/M	Right L2-S2	5 mos	9
10	61/M	Right T4-T6	6 mos	9.5
11	64/M	Left T5-T8	8 mos	9.5

M = male; T = level of thoracic vertebrae; L: level of lumbar vertebrae; S: level of sacral vertebrae.

3.4. The effects of PHN on functional connectivity

To examine the effects of PHN on the functional connectivity associated with pain-related regions (see earlier), we performed SCA.

3.4.1. Intergroup comparison of functional connectivity with left caudate head

In the PHN group as compared with control subjects, dynamic CBF within the left caudate nucleus demonstrated increased correlation with CBF variations in the bilateral thalamic regions, bilateral PCC, right/contralateral lentiform nuclei, left/ipsilateral insula, right/contralateral MPFC, right/contralateral parahippocampal gyrus, and cerebral cortex, including superior parietal lobule, bilateral middle temporal gyri, and bilateral lingual gyri (Fig. 5, Table 4). Conversely, dynamic CBF within this region showed decreased correlation with the right/contralateral MPFCs.

Table 2
Clusters of significant cerebral blood flow increases in patient group.

Regions	Brodmann area	MNI coordinates			T values	K	Absolute cerebral blood flow values (mL/100 g/min)
		X	Y	Z			
Left caudate head		−14	24	2	4.1	102	47.38 ± 3.26
Left lentiform nucleus		−22	−6	18	3.55	796	65.21 ± 3.11
Left insula	13	−36	4	8	3.36	80	67.57 ± 2.40
Right thalamus		18	−6	12	3.44	72	48.44 ± 2.61
Left primary somatosensory cortex	3	−34	−24	40	3.36	80	40.38 ± 3.10
Left primary motor cortex	6	−38	−8	36	3.55	73	41.43 ± 2.12
Left amygdala		−22	−8	−12	3.08	40	50.21 ± 4.1
Left inferior parietal lobular	40	−48	−50	32	3.35	316	48.19 ± 2.91
	39	−44	−74	28	2.85	28	
Right fusiform gyrus	37	44	−38	−18	3.23	72	42.23 ± 2.4
Bilateral superior temporal gyrus	41,39	52	−40	12	3.62	80	65.77 ± 4.72
Bilateral middle temporal gyrus	21,39	−52	−26	−12	3.73	73	52.38 ± 3.51

K = number of voxels in cluster.

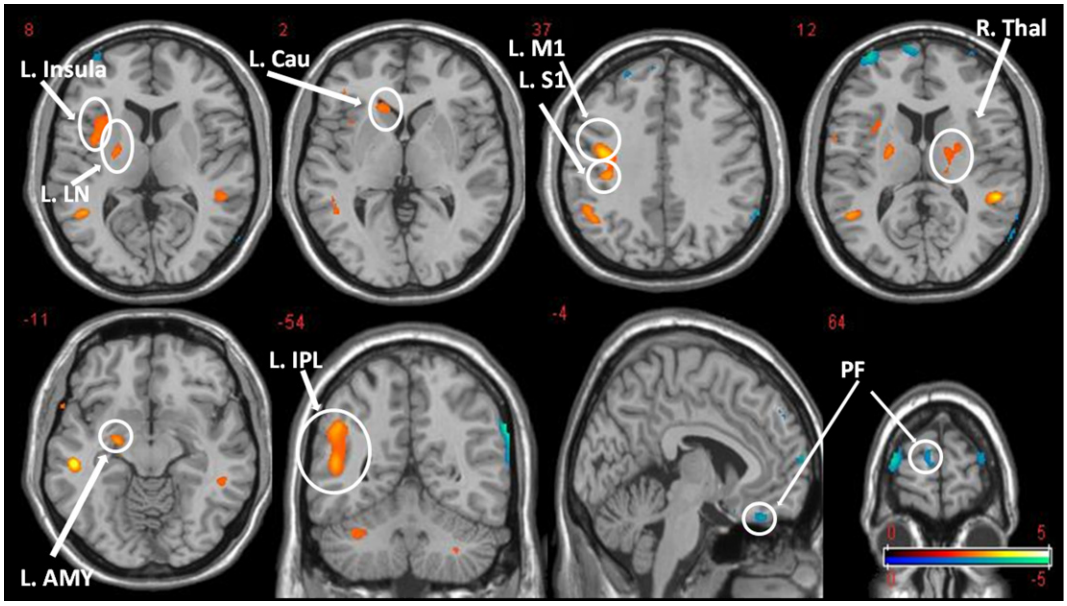

Fig. 3. The effects of PHN on regional cerebral blood flow. Areas of regional cerebral blood flow affected by postherpetic neuralgia have been projected onto the Colin-brain in Montreal Neurological Institute space. The color of each voxel corresponds to its t-value, per the color bar scale. These voxels represent suprathreshold t-statistics (cluster level corrected $P < .05$). A minimum cluster extent of 10 voxels was also applied. LN = lentiform nucleus; Cau = caudate head; M1 = primary motor cortex; S1 = primary somatosensory cortex; Thal = thalamus; AMY = amygdala; IPL = inferior parietal lobular; PF = prefrontal lobes.

Table 3
Clusters of significant cerebral blood flow decreases in patient group.

Regions	Brodmann area	MNI coordinates			T values	K
		X	Y	Z		
Right inferior parietal	40	64	−56	34	4.98	256
lobular	39	58	−68	36	2.74	256
Bilateral superior frontal	8	10	44	52	2.77	21
gyri	10	−8	70	14	4.05	58
Left middle frontal gyrus	10	−34	64	14	4.2	141
Right middle frontal gyrus	47	30	22	−18	2.87	14

K = number of voxels in cluster.

3.4.2. Intergroup comparison of functional connectivity with left S1

In the PHN group as compared with control subjects, dynamic CBF within the left S1 demonstrated increased connectivity with CBF variations in the frontal cortex, such as bilateral superior and middle frontal gyri, as well as left/ipsilateral MPFC. No significantly reduced connectivity was observed (Fig. 6A, Table 5).

3.4.3. Intergroup comparison of functional connectivity with left insula

In the PHN group as compared with control subjects, dynamic CBF within the left insula demonstrated increased connectivity with CBF variations in the bilateral caudate body, right/contralateral insula, and inferior frontal gyrus (Fig. 6B, Table 6). Reduced connectivity in patients has been observed in the right/contralateral temporal cortex.

3.4.4. Intergroup comparison of functional connectivity with right thalamus

In the PHN group as compared with control subjects, dynamic CBF within the right thalamus demonstrated increased connectivity with CBF variations in the left/contralateral thalamus, bilateral lentiform nucleus, left/contralateral caudate head, and inferior temporal gyrus (Fig. 6C, Table 7). No significantly reduced connectivity was observed.

4. Discussion

The aim of our study was to establish the effects of PHN pain on rCBF and functional brain networks. The cohort in our study suffered from chronic pain for less than 2 years and showed significant CBF alterations in several pain-related regions, including the thalamus, insula, striatum, and S1. These results are supported by previous studies based on BOLD fMRI [14]. In addition, the CBF value changes in these 4 areas showed significant positive correlation with pain intensity, strongly suggesting their involvement with PHN pain.

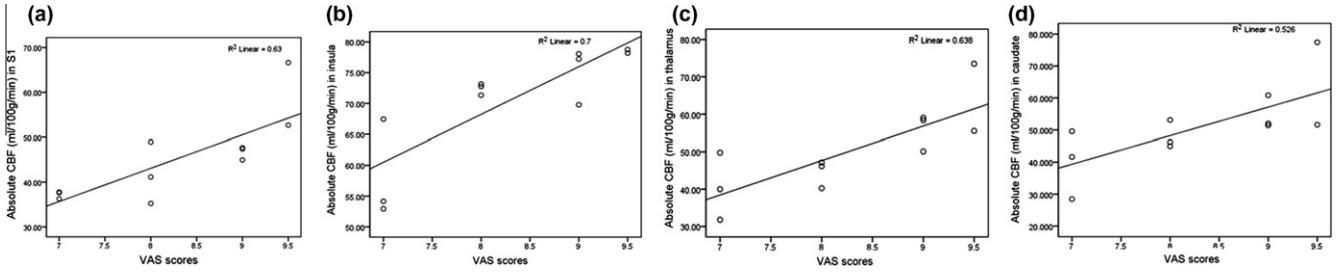

Fig. 4. The relationship between regional cerebral blood flow and pain intensity. Correlation analyses between absolute cerebral blood flow values of left S1, left insula, right thalamus, left caudate head, and pain intensity in patient group. All illustrated results were statistically significant. CBF = cerebral blood flow; VAS = visual analog scale.

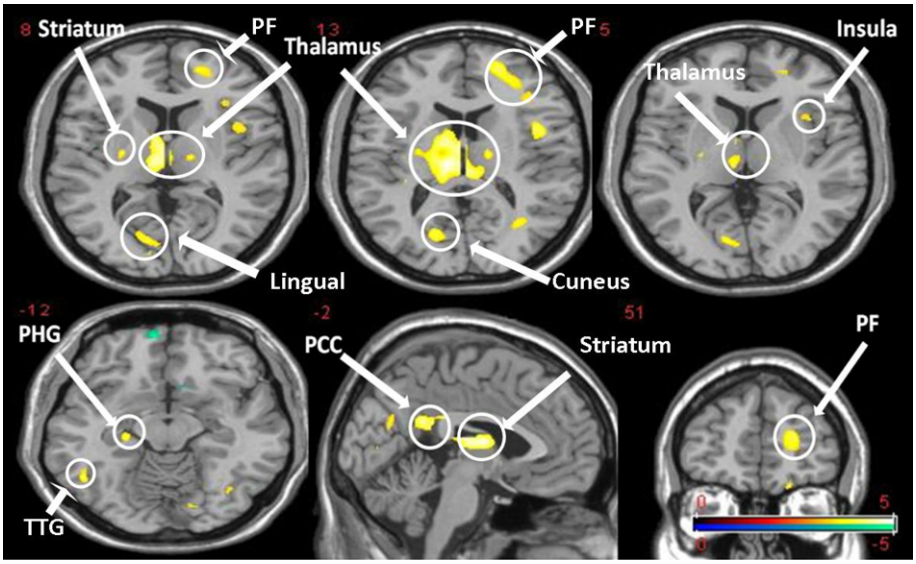

Fig. 5. The effects of postherpetic neuralgia pain on the left caudate head functional connectivity. Representative brain regions showed positive or negative functional connectivity with left caudate head (cluster level corrected $P < .05$). PHG = parahippocampal gyrus; PCC = posterior cingulate cortex; PF = prefrontal lobes; TTG = transverse temporal gyrus; Lingual = lingual gyrus.

Table 4
Brain areas of patients with an increased connectivity with the left caudate nucleus in comparison to healthy subjects.

Regions	Brodmann area	MNI coordinates			T values	K
		X	Y	Z		
Bilateral thalamus		−6	−28	16	5.45	1967
		16	−18	18	5.04	1967
Bilateral posterior cingulate cortex	23	6	−48	24	4.98	1967
	23	−4	−38	22	4.73	1967
Right lentiform nucleus		26	−12	6	4.27	1967
Left insula	13	−44	6	12	4.33	262
Left medial prefrontal cortex	10	−20	52	12	4.25	262
Right parahippocampal gyrus	28	24	−24	−10	4.12	35
Bilateral fusiform gyrus	37,19	−36	−70	−12	3.53	11
Right transverse temporal gyrus	41	34	−34	14	3.92	71
Left superior parietal lobular	7	−34	−48	52	4.14	24
Bilateral lingual gyrus	18	12	−78	6	3.98	221
Right cuneus	18	18	−74	16	4.14	221

K = number of voxels in cluster.

Many studies have investigated the brain activity associated with pain by applying painful stimulation, such as acupuncture [35], or task design such as evoked pain [15]. However, spontaneous pain is a defining trait of neuropathic pain [7]. It has been demonstrated that fMRI signals during the resting state could be used to investigate the intrinsic functional connectivity of the regions modulated by pain [14,22]. Thus, the resting state may reflect the spontaneous components dominating pain processing.

PHN was associated with increased rCBF in numerous regions involved in emotion, sensation, and motor control. The insula, S1, and thalamus have been previously linked to both acute and chronic pain [3,39] and it has been reported that these regions encode sensory discriminative components of acute pain in terms of both intensity and somatotopy [10,11,26]. Additionally, the insula and S1 commonly determinate increased activity in chronic pain [5,17].

In the present study, the severity of PHN was linked to the amount of CBF within the thalamus. This observation is supported by previous reports of increased activity within this region in patients with trigeminal neuralgia [27], complex regional pain syndrome [40], and PHN [14]. Other studies, however, have also linked chronic pain to reduced thalamic blood flow [19,46]. Ushida et al. [40] observed increased CBF within the thalamus in patients with early-stage neuropathic pain (ie, less than 12 months), yet decreased CBF in this region as the disease progressed or after treatment. Together, these observations indicate that the thalamus is closely linked to pain pathogenesis, yet dependent upon the type, severity, and duration of spontaneous pain.

In PHN patients, pain severity was also linked to CBF within the S1 region. The S1 region contributes to the processing of tactile information, as well as the suppression of painful stimuli, and thus seems to play a crucial role in the regulation of neuropathic pain [41]. Similar to previous reports on the effects of diabetic neuropathic pain on brain connectivity [6], the S1 also showed different connectivity within the cerebral cortex in PHN when compared with healthy subjects. These results are supported by the report from Vartiainen et al. [41], which also observed cortical reorganization associated with S1 in patients with unilateral chronic pain evoked by viral infection.

Increased CBF within motor areas such as M1 in patients with chronic pain may reflect suppression of movement [3]. The current results may therefore indicate patient desire to avoid movement-induced pain during the experiment.

The striatum, which receives projections from the entire cerebral cortex [33], has rich connections to sensorimotor, attentional, and limbic emotion-processing networks. Although the striatum is not commonly associated with pain, several studies have linked its activity to chronic pain, including fibromyalgia [34] and complex regional pain syndrome [23]. As a part of the reward, hedonic, and emotional circuitries, the striatum is believed to primarily reflect the spontaneous pain of PHN in BOLD fMRI studies [14,15]. Our results further support its role in chronic PHN pain; ie, in patients as compared with control subjects, it was activated to a greater degree at rest, and more connected to regions associated with both pain (ie, the thalamus, insula, and S1) and emotion (ie, the insula, PCC, and parahippocampal gyrus). We therefore contend that the striatum plays an important role in PHN pain and may serve as a hub for processing of both painful and emotional information.

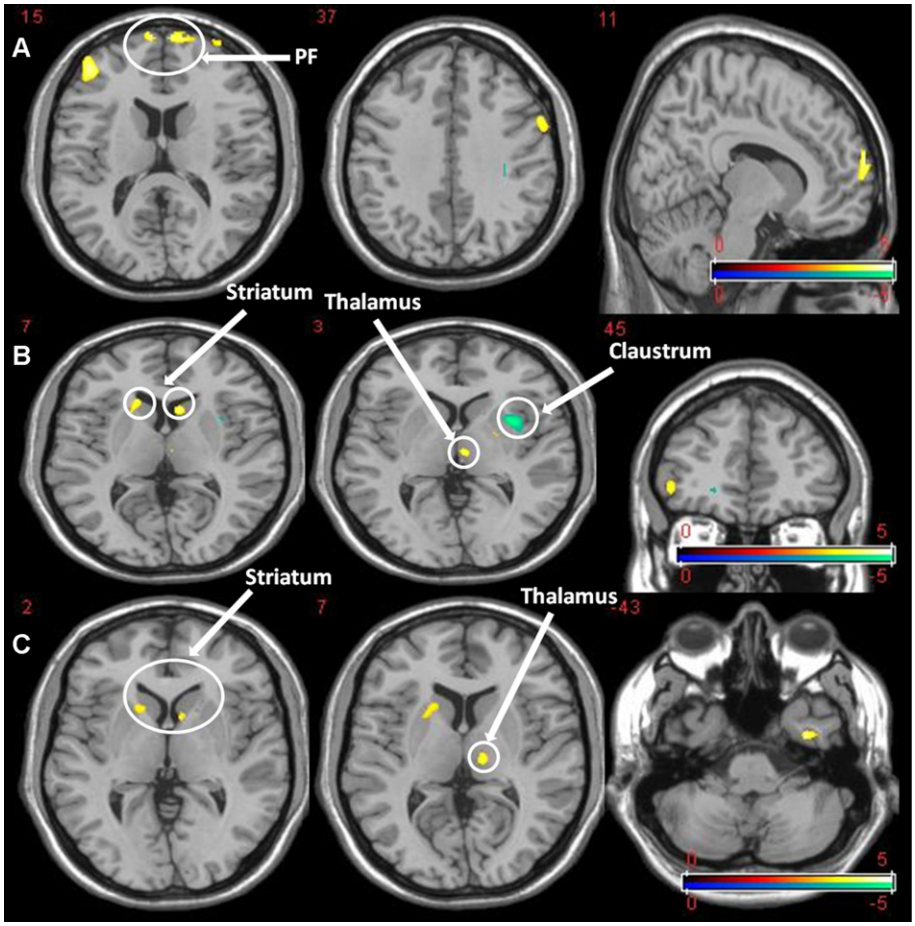

Fig. 6. The effects of postherpetic neuralgia pain on S1, insula, and thalamus functional connectivity. Representative brain regions showing positive or negative functional connectivity with left S1 (A), left insula (B), and right thalamus (C) (cluster level corrected $P < .05$). PF = prefrontal lobes.

Table 5
Brain areas of patients with an increased connectivity with the left primary somatosensory cortex in comparison to healthy subjects.

Regions	Brodmann area	MNI coordinates			T values	K
		X	Y	Z		
Left medial prefrontal cortex	10	−10	66	18	4.55	129
Bilateral middle frontal gyri	46	42	44	10	5.13	203
	10	−58	6	38	4.12	63
Bilateral superior frontal gyri	10	8	66	20	4.4	27
	10	−40	50	20	3.86	10

K = number of voxels in cluster.

Table 6
Brain areas of patients with an increased connectivity with the left insula in comparison to healthy subjects.

Regions	Brodmann area	MNI coordinates			T values	K
		X	Y	Z		
Left thalamus		−4	−16	2	4.13	17
Bilateral caudate body		−8	16	8	4.72	34
		18	20	6	4.02	29
Right insula	6	32	2	22	4.05	22
Right inferior frontal gyrus	46	48	40	−2	4.13	17

K = number of voxels in cluster.

Table 7
Brain areas of patients with an increased connectivity with the right thalamus in comparison to healthy subjects.

Regions	Brodmann area	MNI coordinates			T values	K
		X	Y	Z		
Left thalamus		−10	−20	6	4.83	167
Bilateral lentiform nucleus		−28	0	10	4.55	56
		16	8	2	4.01	21
Left caudate head		−8	6	2	3.77	14
Left inferior temporal gyrus	20	−44	−4	−40	4.58	48

K = number of voxels in cluster.

In the current study, CBF within the anterior cingulate cortex (ACC) and prefrontal cortices was not affected by PHN. Previous studies have indicated that both of these regions are modulated by pain unpleasantness rather than pain intensity [18,36]. Moreover, multiple studies have demonstrated that the ACC is activated in response to evoked pain [8], acute pain, and visceral pain [18]. The lack of involvement in these regions in PHN patients may therefore represent differences in the processing of chronic and acute pain.

Although changes in ACC activation in PHN patients after lidoderm therapy have been reported by Geha et al. [14], the discrepancies between the 2 studies include different fMRI techniques and group comparisons. BOLD fMRI, which was used in a previous study, obtained a higher SNR than ASL-CBF, so more regions with a significant difference might be detected by BOLD. In addition,

treatments such as lidoderm can not only relieve pain intensity but also ease unpleasantness that is modulated by ACC. Thus, further experiment with treatments should be explored in the future.

Pain perception is believed to emerge from the integration of information among multiple brain regions, and thus lends itself well to connectivity analyses [7]. By studying the functional connectivity associated with those regions linked to PHN pain, we have begun to establish the network involved in processing chronic pain. Specifically, using dynamic CBF analysis, 3 circuits involved in PHN pain were identified. The first circuit included connections among the striatum, insula, and thalamus (see Figs. 5 and 6). This functional network may indicate a greater interaction among the 3 pain-related regions under PHN pain for transporting neurotransmitters. The second circuit included the frontal cortical-basal ganglia-thalamic-cerebral cortical pathway [16], in which the striatum and thalamus were crucial components. This circuit mediates motivation and emotional drive, thereby facilitating development and expression of goal-directed behaviors [16]. The third circuit included components of the brain's reward circuitry, including the striatum, prefrontal cortex, amygdala, and parahippocampal gyrus, which indicates that PHN pain may be accompanied by strong emotional involvement [5,7].

The regions with PHN-related CBF change were located primarily in the left cerebral hemisphere. This observation may be due to several factors, including the inclusion of only right-handed (ie, left-hemisphere-dominant) subjects and/or the fact that 9 of 11 patients presented with left-side lesions. Future studies are therefore warranted to examine the effects of handedness and lesion side on rCBF in this population.

Quantitative CBF measurements showed its ability in locating and monitoring pain-sensitive brain regions. By measuring and comparing resting-state CBF values before and after drug administration, ASL could be used to study the drug effects responding to painful stimuli [31,38]. Thus, ASL may enable fMRI to become a potential strategy for objectively evaluating painful information in the clinic [21].

For the dynamic ASL analysis, functional connectivity is fundamentally a correlation between 2 time courses, and thus is dependent on the time delay. To address this problem, we first used QUIPSS II to generate variable TIs between different imaging slices to reduce the effects of transit delays. Second, we also considered slice timing during the CBF calculation procedure to compensate for acquisition time differences between slices.

Our study had several limitations. First, because all PHN patients were under constant pain with limited variability, we were unable to determine intrasubject correlations between CBF and pain intensity. Second, an age gap still existed in both the patient and the control groups. However, correlation analyses between CBF changes of related regions and age revealed no significance ($|r| < 0.3$, $P > .5$). Third, SCA cannot determine the direction of the interregional influences. Future studies may therefore gain further insight into the neural alterations associated with neuropathic pain by using Granger causality analysis, which overcomes this drawback by using multivariate autoregressive modeling.

In conclusion, this study used ASL fMRI and examined both static and dynamic CBF to identify the specific brain regions and circuits associated with PHN pain. Within PHN patients, rCBF in the left striatum, left insula, left S1, and right thalamus were highly correlated with pain intensity. We also observed that a characteristic network of brain connectivity, which included the striatum, thalamus, and insula, played an important role in the processing of PHN pain. These results may therefore be used to help improve the management and treatment of the often-debilitating symptoms of PHN.

Conflict of interest statement

The authors declare no conflict of interest.

Acknowledgements

The authors thank all of the volunteers who participated in this study, Professor Eric Wong for his technical support, Drs. Meng Li and Alexander Merkle for their grammar corrections to this paper, and Dr. Zhang Yong in GE Healthcare for his help in technique consultation. Our study was supported by "the Fundamental Research Funds for the Central Universities".

References

[1] Acerra NE, Moseley GL. Dysynchiria: watching the mirror image of the unaffected limb elicits pain on the affected side. Neurology 2005;65:751–3.
[2] Aguirre GK, Detre JA, Zarahn E, Alsop DC. Experimental design and the relative sensitivity of BOLD and perfusion fMRI. Neuroimage 2002;15:488–500.
[3] Apkarian AV, Bushnell MC, Treede RD, Zubieta JK. Human brain mechanisms of pain perception and regulation in health and disease. Eur J Pain 2005;9:463–84.
[4] Apkarian AV, Sosa Y, Krauss BR, Thomas PS, Fredrickson BE, Levy RE, Harden RN, Chialvo DR. Chronic pain patients are impaired on an emotional decision-making task. PAIN® 2004;108:129–36.
[5] Baliki MN, Geha PY, Apkarian AV, Chialvo DR. Beyond feeling: chronic pain hurts the brain, disrupting the default-mode network dynamics. NeuroImage 2008;28:1398–403.
[6] Cauda F, Sacco K, Agata FD, Duca S, Cocito D, Geminiani G, Migliorati F, Isoardo G. Low-frequency BOLD fluctuations demonstrate altered thalamocortical connectivity in diabetic neuropathic pain. BMC Neurosci 2009;14:1–14.
[7] Cauda F, Sacco K, Duca S, Cocito D, D'Agata F, Geminiani GC, Canavero S. Altered resting state in diabetic neuropathic pain. PLoS One 2009;4:e4542.
[8] Christmann C, Koeppe C, Braus DF, Ruf M, Flor H. A simultaneous EEG-fMRI study of painful electric stimulation. Neuroimage 2007;34:1428–37.
[9] Coghill RC, Sang CN, Maisog JM, Iadarola MJ. Pain intensity processing within the human brain: a bilateral, distributed mechanism. J Neurophysiol 1999;82:1934–43.
[10] Davis KD, Kwan CL, Crawley AP, Mikulis DJ. Functional MRI study of thalamic and cortical activations evoked by cutaneous heat, cold, and tactile stimuli. J Neurophysiol 1998;80:1533–46.
[11] Derbyshire SW, Jones AK, Gyulai F, Clark S, Townsend D, Firestone LL. Pain processing during three levels of noxious stimulation produces differential patterns of central activity. PAIN® 1997;73:431–45.
[12] Detre JA, Wang J, Wang Z, Rao H. Arterial spin-labeled perfusion MRI in basic and clinical neuroscience. Curr Opin Neurol 2009;22:348–55.
[13] Folstein MF, Folstein SE, McHugh PR. "Mini-mental state": a practical method for grading the cognitive state of patients for the clinician. J Psychiatr Res 1975;12:189–98.
[14] Geha PY, Baliki MN, Chialvo DR, Harden RN, Paice JA, Apkarian AV. Brain activity for spontaneous pain of postherpetic neuralgia and its modulation by lidocaine patch therapy. PAIN® 2007;128:88–100.
[15] Geha PY, Baliki MN, Wang X, Harden RN, Paice JA, Apkarian AV. Brain dynamics for perception of tactile allodynia (touch-induced pain) in postherpetic neuralgia. PAIN® 2008;138:641–56.
[16] Gopinath K, Ringe W, Goyal A, Carter K, Dinse HR, Haley R, Briggs R. Striatal functional connectivity networks are modulated by fMRI resting state conditions. NeuroImage 2010;54:380–8.
[17] Gracely RH, Geisser ME, Giesecke T, Grant MA, Petzke F, Williams DA, Clauw DJ. Pain catastrophizing and neural responses to pain among persons with fibromyalgia. Brain 2004;127:835–43.
[18] Hofbauer RK, Rainville P, Duncan GH, Bushnell MC. Cortical representation of the sensory dimension of pain. J Neurophysiol 2001;86:402–11.
[19] Iadarola MJ, Max MB, Berman KF, Byas-Smith MG, Coghill RC, Gracely RH, Bennett GJ. Unilateral decrease in thalamic activity observed with positron emission tomography in patients with chronic neuropathic pain. PAIN® 1995;63:55–64.
[20] Jung BF, Johnson RW, Griffin DR, Dworkin RH. Risk factors for postherpetic neuralgia in patients with herpes zoster. Neurology 2004;62:1545–51.
[21] Kong J, Gollub RL, Rosman IS, Webb JM, Vangel MG, Kirsch I, Kaptchuk TJ. Brain activity associated with expectancy-enhanced placebo analgesia as measured by functional magnetic resonance imaging. J Neurosci 2006;26:381–8.
[22] Kong J, Tu P-C, Zyloney C, Su T-P. Intrinsic functional connectivity of the periaqueductal gray, a resting fMRI study. Behav Brain Res 2010;211:215–9.
[23] Lebel A, Becerra L, Wallin D, Moulton EA, Morris S, Pendse G, Jasciewicz J, Stein M, Aiello-Lammens M, Grant E, Berde C, Borsook D. FMRI reveals distinct CNS processing during symptomatic and recovered complex regional pain syndrome in children. Brain 2008;131:1854–79.
[24] Liu TT, Brown GG. Measurement of cerebral perfusion with arterial spin labeling: Part 1. Methods. J Int Neuropsychol Soc 2007;13:517–25.

[25] Liu TT, Wong EC. A signal processing model for arterial spin labeling functional MRI. Neuroimage 2005;24:207–15.
[26] Mayer EA, Berman S, Suyenobu B, Labus J, Mandelkern MA, Naliboff BD, Chang L. Differences in brain responses to visceral pain between patients with irritable bowel syndrome and ulcerative colitis. PAIN® 2005;115:398–409.
[27] Moisset X, Villain N, Ducreux D, Serrie A, Cunin G, Valade D, Calvino B, Bouhassira D. Functional brain imaging of trigeminal neuralgia. Eur J Pain 2011;15:124–31.
[28] Oaklander AL. The density of remaining nerve endings in human skin with and without postherpetic neuralgia after shingles. PAIN® 2001;92:139–45.
[29] Ohara S, Crone NE, Weiss N, Lenz FA. Analysis of synchrony demonstrates 'pain networks' defined by rapidly switching, task-specific, functional connectivity between pain-related cortical structures. PAIN® 2006;123:244–53.
[30] Owen DG, Clarke CF, Ganapathy S, Prato FS, St Lawrence KS. Using perfusion MRI to measure the dynamic changes in neural activation associated with tonic muscular pain. PAIN® 2010;148:375–86.
[31] Owen DG, Thomas AW, Prato FS, Lawrence KSS. Quantification of pain-induced changes in cerebral blood flow by perfusion MRI. PAIN® 2008;136:85–96.
[32] Peyron R, Laurent B, Garcia-Larrea L. Functional imaging of brain responses to pain. A review and meta-analysis. Neurophysiol Clin 2000;30:263–88.
[33] Postuma RB, Dagher A. Basal ganglia functional connectivity based on a metaanalysis of 126 positron emission tomography and functional magnetic resonance imaging publications. Cereb Cortex 2006;16:1508–21.
[34] Pujol J, López-Solà M, Ortiz H, Vilanova JC, Harrison BJ, Yücel M, Soriano-Mas C, Cardoner N, Deus J. Mapping brain response to pain in fibromyalgia patients using temporal analysis of FMRI. PLoS One 2009;4:e5224.
[35] Qin W, Tian J, Bai L, Pan X, Yang L, Chen P, Dai J, Ai L, Zhao B, Gong Q, Wang W, von Deneen KM, Liu Y. FMRI connectivity analysis of acupuncture effects on an amygdala-associated brain network. Mol Pain 2008;13:4–55.
[36] Rainville P, Duncan GH, Price DD, Carrier B, Bushnell MC. Pain affect encoded in human anterior cingulated but not somatosensory cortex. Science 1997;277:968–71.
[37] Rao H, Wang J, Giannetta J, Korczykowski M, Shera D, Avants BB, Gee J, Detre J, Hurt H. Altered resting cerebral blood flow in adolescents with in utero cocaine exposure revealed by perfusion functional MRI. Pediatrics 2007;120:1245–54.
[38] Rogers R, Wise RG, Painter DJ, Longe SE, Tracey I. An investigation to dissociate the analgesic and anesthetic properties of ketamine using functional magnetic resonance imaging. Anesthesiology 2004;100:292–301.
[39] Singer T, Seymour B, O'Doherty J, Kaube H, Dolan RJ, Frith CD. Empathy for pain involves the affective but not sensory components of pain. Science 2004;303:1157–62.
[40] Ushida T, Fukumoto M, Binti C, Ikemoto T, Taniguchi S, Ikeuchi M, Nishihara M, Tani T. Alterations of contralateral thalamic perfusion in neuropathic pain. Open Neuroimaging J 2010;24:182–6.
[41] Vartiainen N, Kirveskari E, Kallio-Laine K, Kalso E, Forss N. Cortical reorganization in primary somatosensory cortex in patients with unilateral chronic pain. J PAIN® 2009;10:854–9.
[42] Wang Z, Aguirre GK, Rao H, Wang JJ, Childress AR, Detre JA. Empirical ASL data analysis using an ASL data processing toolbox: ASLtbx. Magn Reson Imaging 2008;26:261–9.
[43] Wang Z, Wang J, Connick TJ, Wetmore GS, Detre JA. Continuous ASL (CASL) perfusion MRI with an array coil and parallel imaging at 3 T. Magn Reson Med 2005;54:732–7.
[44] Wong EC, Buxton RB, Frank LR. Implementation of quantitative perfusion imaging techniques for functional brain mapping using pulsed arterial spin labeling. NMR Biomed 1997;10:237–49.
[45] Wong EC, Buxton RB, Frank LR. Quantitative imaging of perfusion using a single subtraction (QUIPSS and QUIPSS II). Magn Reson Med 1998;39:702–8.
[46] Wu CT, Fan YM, Sun CM, Borel CO, Yeh CC, Yang CP, Wong CS. Correlation between changes in regional cerebral blood flow and pain relief in complex regional pain syndrome type 1. Clin Nucl Med 2006;31:317–20.
[47] Ye FQ, Berman KF, Ellmore T, Esposito G, van Horn JD. H215O PET validation of steady-state arterial spin tagging cerebral blood flow measurements in humans. Magn Reson Med 2000;44:450–6.
[48] Zou Q, Wu CW, Stein EA, Zang Y, Yang Y. Static and dynamic characteristics of cerebral blood flow during the resting state. Neuroimage 2009;48:515–24.